

## **AGRP neurons are sufficient to orchestrate feeding behavior rapidly and without training**

**Yexica Aponte, Deniz Atasoy, and Scott M. Sternson\***

Howard Hughes Medical Institute, Janelia Farm Research Campus, 19700 Helix Dr. Ashburn, VA 20147, USA

### **Abstract**

Two intermingled hypothalamic neuron populations, specified by expression of agouti-related peptide (AGRP) or pro-opiomelanocortin (POMC), positively and negatively influence feeding behavior respectively, possibly by reciprocally regulating downstream melanocortin receptors. However, the sufficiency of these neurons to control behavior, and the relationship of their activity to the magnitude and dynamics of feeding are unknown. To measure this, we used channelrhodopsin-2 for cell type-specific photostimulation. Activation of only 800 AGRP neurons in mice evoked voracious feeding within minutes. The behavioral response increased with photoexcitable neuron number, photostimulation frequency, and stimulus duration. Conversely, POMC neuron stimulation reduced food intake and body weight, which required melanocortin receptor signaling. However, AGRP neuron-mediated feeding was not dependent on suppressing this melanocortin pathway, indicating that AGRP neurons directly engage feeding circuits. Furthermore, feeding was evoked selectively over drinking without training or prior photostimulus exposure, which suggests that AGRP neurons serve a dedicated role coordinating this complex behavior.

---

Multiple neuron populations distributed throughout the brain influence the decision to seek and consume food<sup>1</sup>. AGRP neurons are thought to positively regulate feeding behavior because AGRP<sup>2</sup> and a co-expressed peptide, neuropeptide Y (NPY)<sup>3–5</sup>, increase food intake when injected into the brain. Moreover, AGRP neuron firing rate is elevated in brain slices from food-deprived mice<sup>6</sup>. In contrast, genetic and pharmacologic evidence suggest that POMC neurons inhibit feeding by releasing  $\alpha$ -melanocyte stimulating hormone, a melanocortin receptor agonist<sup>7,8</sup>. Both of these populations are located in the hypothalamic arcuate nucleus (ARC). Within the ARC, AGRP neurons inhibit POMC neurons<sup>9,10</sup>. Also, AGRP directly blocks melanocortin receptors<sup>2</sup>. Thus, AGRP neurons have been proposed to serve a modulatory function, counter-regulating the melanocortin pathway to reduce satiety and promote food intake<sup>11</sup>.

---

Users may view, print, copy, download and text and data-mine the content in such documents, for the purposes of academic research, subject always to the full Conditions of use: [http://www.nature.com/authors/editorial\\_policies/license.html#terms](http://www.nature.com/authors/editorial_policies/license.html#terms)

\*Correspondence should be addressed to S.M.S. (sternsons@janelia.hhmi.org).

#### **AUTHOR CONTRIBUTIONS**

Y.A. performed the behavioral experiments and D.A. performed and analyzed electrophysiological experiments. Y.A. and S.M.S. designed the study, analyzed the data, and wrote the paper.

#### **COMPETING INTERESTS**

The authors declare no competing interests.

However, loss-of-function experiments, which showed that AGRP neuron ablation in adult mice leads to anorexia<sup>12</sup>, could not be explained by disinhibition of melanocortin signaling<sup>13</sup>. Instead, starvation was proposed to result from severe gastrointestinal malaise<sup>14</sup>, and food intake could be permanently rescued by benzodiazepine treatment<sup>14</sup>. Thus, it is unclear whether AGRP neurons directly control feeding or if, instead, their role is permissive, either preventing a state of intense nausea or suppressing melanocortin signaling. This distinction raises the question of whether AGRP neuron activity is sufficient to evoke feeding behavior, and if so, whether suppression of melanocortin signaling is required for this. To address these issues, we sought to directly determine the role of these neurons for feeding by rapidly and cell type-selectively increasing their electrical activity.

## RESULTS

### Cell type specific neuron activation

To overcome cell type heterogeneity in the ARC, which contains AGRP, POMC, and several other cell populations, we used light to selectively stimulate either AGRP or POMC neurons. The light-activated cation channel channelrhodopsin-2 (ChR2)<sup>15,16</sup>, fused to the fluorophore tdtomato (ChR2:tdtomato), was targeted to AGRP or POMC neurons by injecting the Cre recombinase-dependent viral vector rAAV-FLEX-*rev*-ChR2:tdtomato<sup>17</sup> into the ARC of *agrp-cre*<sup>18</sup> and *pomc-cre*<sup>19</sup> transgenic mice, rendering these neurons photoexcitable. The cell type selectivity of this viral approach and the ChR2-dependent photoexcitability of these cell populations have been demonstrated previously<sup>17</sup>.

For light delivery, an optical fiber was targeted to the dorsal portion of the hypothalamus in mice expressing ChR2:tdtomato in AGRP neurons (AGRP-ChR2 mice; Fig. 1a). Animals were tested for optically-evoked feeding behavior during the early light period when mice normally eat little. Although AGRP neuron activity *in vivo* is unknown, optogenetic techniques can map the relationship between patterns of activity and behavior. We began by stimulating AGRP neurons with bursts of light pulses (20 Hz, 1 s), separated by 3 seconds, and repeated over 1 hour (Fig. 1b). In brain slice experiments, we found that a similar stimulation protocol could drive firing in AGRP neurons over extended time scales (Supplementary Fig. 1). This stimulus pattern is similar to activity patterns evoked in AGRP neurons by orexigenic hormones and neuropeptides applied to brain slices<sup>20</sup>.

### AGRP neurons are sufficient to induce voracious feeding

Within minutes, AGRP-ChR2 mice ate voraciously in response to photostimulation without training or prior exposure to the stimulus (Fig. 1c). Food intake was unchanged in photostimulated *agrp-cre* mice that were not infected with rAAV-FLEX-*rev*-ChR2:tdtomato (Fig. 1c). Because the stimulus was applied to well-fed mice during the early light period, these results show that AGRP neuron activity is not just permissive for feeding but, instead, is sufficient to orchestrate feeding even under physiological, circadian, and hypothalamic gene expression conditions that are typically associated with satiety. However, it was unclear whether AGRP neurons serve simply as a switch for feeding behavior, in which case food intake would be expected to rise discontinuously following sufficient neuron activation. Alternatively, the intensity of feeding behavior could be closely tied to the level

and duration of neuron activity, which would lead to a graded, continuous increase in feeding with increasing AGRP neuron activity. To address these possibilities, we investigated the relationship of externally imposed neuron activity to the magnitude and dynamics of the behavioral response.

The magnitude of food intake showed an increasing relationship with the number of ChR2-expressing neurons (Fig. 1d). In mice with zero or less than 100 ChR2-expressing neurons, no evoked feeding was observed (Fig. 1e). Photostimulated mice with 300 – 700 ChR2-expressing neurons consumed significantly more food (Fig. 1f). For mice with more than 800 ChR2-expressing neurons, feeding responses were still greater and mice were effectively at maximal levels of consumption (for greater than 800 neurons, neurons vs. food intake, linear least squares goodness of fit:  $r^2 = 0.06$ ). Furthermore, evoked food intake was nearly as large as re-feeding after 24 hour food deprivation (1 hour intake, stimulated:  $0.85 \pm 0.06$  g; re-fed after fasting:  $1.04 \pm 0.06$  g; Fig. 1f). After photostimulation was terminated, feeding returned to pre-stimulus levels (Fig. 1e). Notably, consumption elicited by AGRP neuron activation was directed towards food and not water, which was freely available in the cage. All mice for which water consumption was recorded ate before drinking in response to photostimulation (12/12 mice), and drinking was not initiated until  $13.0 \pm 0.9$  min after feeding started. Also, the feeding response magnitude did not appear to be related to a specific distribution of ChR2-expressing AGRP neurons along the rostral-caudal length on the ARC (Supplementary Fig. 2). Because feeding increased with the number of ChR2-expressing AGRP neurons (Fig. 1f), this indicates that AGRP neuron activity produces a signal to which there is a proportional and behaviorally-specific food-directed response. To explore this further, we considered the effect of different AGRP neuron stimulation patterns.

### Evoked feeding depends on photostimulus frequency

We tested the dependence of food intake on stimulus frequency using two protocols. On subsequent days, the stimulus frequency was varied between 20, 10, and 2 Hz, followed by a return to 20 Hz (stimulus protocol 1; Fig. 2a). Under these conditions, food intake during photostimulation was significantly increased relative to the pre-stimulus period (Supplementary Fig. 3a-d), and consumption diminished with decreasing stimulus frequency (Fig. 2b). Notably, for each mouse, feeding during the second 20 Hz stimulation trial was similar to the amount consumed in the initial trial despite variability in consumption across individual subjects (linear least squares fit for consumption in trial 1 vs. trial 2: slope = 0.81;  $r^2 = 0.70$ ; Supplementary Fig. 3e), demonstrating that evoked food consumption is consistent across subsequent trials of AGRP neuron activation.

Because this protocol also reduced the number of light pulses in the brain as the stimulus frequency was decreased, we sought to distinguish whether these results were due to the reduced number of photostimuli or if AGRP neuron-evoked food intake was frequency dependent. To test this, we delivered 20 light pulses every 10 s such that 20 and 2.5 Hz stimulation frequencies could be applied while maintaining the same number of stimuli over the 1 hour stimulation epoch (stimulus protocol 2; Fig. 2c). In this case, consumption still decreased significantly with stimulation frequency (Fig. 2d). Thus, bursts of AGRP neuron activity influence feeding behavior most effectively.

## Dynamics of light-evoked feeding

Although AGRP neurons have been associated with long-term regulation of energy homeostasis, the rapid manipulation of neuron activity used here enabled investigation of the short-term dynamics of AGRP neuron-mediated feeding. The latency to food consumption with photostimulation of AGRP-ChR2 mice was dependent on the number of infected neurons (Fig. 3a). Mice with greater than 800 ChR2-expressing AGRP neurons and no prior exposure to photostimulation showed an average latency to consumption of  $6.1 \pm 0.9$  min (range: 1.9 – 13.8 min). Mice with intermediate numbers of ChR2-expressing neurons (300 – 700 neurons) had significantly longer latencies to food consumption ( $33.6 \pm 1.5$  min), which is analogous to the moderate consumption observed in these mice. Once food intake was initiated, an early bout of avid feeding was typically followed by smaller bouts of various sizes (Fig. 3b). We calculated feeding bouts by analysis of the inter-pellet intervals (IPIs)<sup>21,22</sup> to determine a bout threshold ( $IPI_{\text{thresh}} = 2.4$  min; see Methods and Supplementary Figs. 4–6), which showed that the mean duration of the first bout was  $11.6 \pm 0.8$  min, during which  $28.1 \pm 1.6$  food pellets were consumed. Bout termination has typically been attributed to the onset of short-term satiety cues<sup>21</sup> such as stomach distension or hormonal signals. Notably, most mice resumed food intake later during the photostimulation epoch, possibly reflecting a balance between AGRP neuron activity and satiety signals.

Because feeding is a complex behavior that involves motivational, sensory, and motor circuits, we investigated whether AGRP neuron activity was only a trigger that initiates a self-propagating feeding response or if continuous photostimulation was required to sustain consumption. To test this, we measured the time scale over which food intake ceased after stimulation was terminated during the first feeding bout. Mice were photostimulated until 5 minutes after the first food pellet was taken, which is less than half of the average first bout duration for continuously stimulated mice. As expected, consumption was maintained throughout the stimulation period, however first bout duration ( $7.3 \pm 1.3$  min; Fig. 3c), first bout consumption ( $18.3 \pm 3.8$  pellets; Fig. 3d), and total food consumption over 1 hour ( $21.2 \pm 4.0$  pellets; Fig. 3d) were significantly less than with continuous stimulation. Also, in mice stimulated for only 5 minutes after taking the first pellet, total food consumption over 1 hour was not significantly different than during the first bout, while in mice continuously stimulated for 1 hour, total food intake was significantly greater relative to the first bout, which is due to intake resulting from subsequent photostimulation-evoked bouts (Fig. 3b,d). These results demonstrate that AGRP neuron-evoked feeding behavior, once initiated, must be sustained by ongoing stimulation, and most mice (4/6) quickly stopped feeding after the offset of the stimulus. Nevertheless, we find that, even in this initial bout, the feeding is not strictly photostimulus-bound. Food intake is proportional to the photostimulus but, for some AGRP-ChR2 mice (2/6), consumption extended beyond the photostimulation for several minutes (Supplementary Fig. 6), indicating that the participation of efferent circuits sustaining food intake can continue for a short time after AGRP neuron stimulation is terminated.

## POMC neurons suppress feeding and body weight

One downstream component of this circuit is POMC neurons, which are inhibited by AGRP neurons, and we sought to test whether suppression of POMC neuron-mediated melanocortin signaling was the pathway through which photostimulated AGRP neurons evoked feeding behavior. For this, we first determined if activating POMC neurons was sufficient to reduce food intake. In brain slice experiments, photostimulation of ChR2-expressing POMC neurons using protocol 1 (20 Hz) reliably drove POMC neuron firing (Supplementary Fig. 7). This stimulus, applied at the transition to the dark period in *ad libitum* fed mice (see Methods), did not significantly affect feeding over the two hours straddling dark period onset (baseline:  $0.32 \pm 0.03$  g; photostimulated:  $0.26 \pm 0.04$  ;  $n = 9$ ; paired *t*-test,  $P = 0.30$ ). However, applying this stimulus pattern for 24 hours significantly reduced food intake by 39% (Fig. 4a) and body weight by 7% (Fig. 4b). Applying light pulses in *pomc-cre* mice lacking ChR2 expression did not significantly change in food intake over 24 hours (107%, paired *t*-test,  $P = 0.43$ ; Fig. 4c). Furthermore, POMC neuron stimulation in  $A^y$  mice, where the ectopically expressed *agouti* protein constitutively blocks melanocortin receptors<sup>23</sup>, did not show reduced feeding (Fig. 4d), thus POMC neuron-mediated hypophagia required melanocortin receptor signaling. Notably, this requirement for melanocortin receptor signaling indicates that other POMC neuron-derived neurotransmitters and neuropeptides, such as the anorexigenic peptide cocaine and amphetamine-related transcript (CART)<sup>24 25</sup>, are not sufficient to reduce *ad libitum* food intake under these conditions.

## Evoked feeding does not require melanocortin suppression

Because POMC neurons required melanocortin signaling to induce hypophagia, which was completely blocked by the  $A^y$  mutation, we tested whether AGRP neuron-evoked food intake was due to suppression of this POMC neuron-mediated pathway by stimulating AGRP neurons in  $A^y$  mice. In these mice, food intake was strongly activated in response to photostimulation (Fig. 5) and was similar to that observed in photostimulated AGRP-ChR2 mice (Fig. 1e). In addition, the latency to consumption of the first pellet was also comparable to response latencies in AGRP-ChR2 mice ( $6.2 \pm 2.0$  min,  $n = 7$ ). These results complement a report that anorexia from AGRP neuron ablation is not rescued by melanocortin blockade<sup>13</sup> and demonstrate that inhibition of melanocortin output by AGRP neurons is not a necessary condition for acutely evoked feeding behavior.

## DISCUSSION

In this study, we explored the causal relationship between cell type-specific neuron activation and feeding behavior for AGRP and POMC neurons in the hypothalamic arcuate nucleus. Our results show that simple stimulus patterns in AGRP neurons are sufficient to rapidly induce the complex behavioral sequences required to seek and consume food. AGRP neuron stimulation was not simply a trigger for feeding; instead, we report multiple lines of evidence indicating that the level of AGRP neuron activity is integral to the magnitude, dynamics, and duration of evoked feeding. We find greater food consumption and a decreasing latency to eat with increasing numbers of photoexcitable neurons. Also, food intake is reduced as the stimulus frequency is decreased, consistent with a graded behavioral

response to different neuron activities. Finally, continuation of evoked feeding requires ongoing stimulation of AGRP neurons, which suggests that activity in downstream circuits is tied to AGRP neuron signaling during the behavior. Such measurements were not previously accessible without genetically encoded tools for cell type-specific, temporally precise manipulation of neuron activity. Together, these experiments show a close relationship of AGRP neuron signaling with downstream circuits that influence the diverse sensory, motor, and motivational components that underlie this behavior.

Selective stimulation of POMC neurons gave the opposite behavioral outcome, reducing food intake and body weight over 24 hours of continuous photostimulation, an effect which required signaling through melanocortin receptors. However, in contrast to pharmacological studies with melanocortin receptor agonists<sup>26,27</sup>, POMC neuron stimulation for two hours straddling dark period onset did not reduce food intake. This difference likely stems from the constraints associated with activation of intrinsic neurons as compared to intracranial injection of a neuromodulator. Specifically, the axon projections of a neuron and the natural expression level of an endogenous neuromodulator limit its distribution and the amount available to interact with downstream receptors. Another aspect of selective neuron activation is that it allows the contribution of other co-released substances to be measured. For POMC neurons, no effect on *ad libitum* feeding behavior was observed with melanocortin receptors blocked in *A<sup>y</sup>* mice, indicating that co-released modulators and neurotransmitters were not sufficient to inhibit food intake under our experimental conditions.

Because the melanocortin pathway regulates feeding behavior, AGRP suppression of POMC-derived melanocortin signaling has been widely considered as a pathway through which these neurons could rapidly increase feeding behavior<sup>11</sup>. However, although these cell populations interact, we find that inhibition of melanocortin receptors is not necessary for an acute AGRP neuron-evoked feeding response. While these photostimulation experiments do not exclude a role for this pathway to regulate food intake over time scales longer than we have investigated here, they demonstrate the capability of AGRP neurons to independently engage other downstream circuits that coordinate feeding. Future experiments could focus on the signaling pathways necessary for evoked feeding, which are likely mediated by other co-released components of AGRP neurons such as the neuromodulator NPY and the fast neurotransmitter  $\gamma$ -aminobutyric acid<sup>14</sup>.

A striking property of AGRP neurons was the capacity for simple photostimulus patterns to drive feeding behavior selectively without training or prior exposure to AGRP neuron stimulation. Previous experiments have shown that simple activity patterns played into cortical neurons could be used to train a behavioral task or activate a learned behavior<sup>28,29</sup>. In other studies, stimulation of molecularly-defined populations conditioned a place preference<sup>30</sup>, reduced latency to waking<sup>31</sup>, and elevated respiration<sup>32</sup>. However, the capability of a small molecularly-defined neuron population to generate a goal-directed behavior without training has not been previously described. One explanation for this result is that AGRP neurons have a dedicated role for controlling feeding behavior and that these exogenously applied activity patterns can substitute for patterns observed during normal activation of these neurons, for example in a state of energy deficit. While natural activity

patterns in behaving animals are not known for AGRP neurons, optogenetic techniques allowed us to probe the capacity of these neurons and their downstream signaling pathways to influence feeding behavior, which showed that a range of activity patterns were sufficient to activate a proportional feeding response.

Thus, these neurons, which transduce circulating signals of metabolic state such as leptin, ghrelin, and glucose<sup>33</sup> into electrical activity, act as interoceptive sensory neurons which can control feeding behavior and may contribute to mediating the internal representation of hunger. Analogous to externally oriented sensory systems where anatomical and functional properties of sensory neurons have facilitated elucidation of neural pathways responsible for sensation and perception, the axon projections of AGRP neurons<sup>34</sup> may guide the identification of the motivational, hedonic, and autonomic circuits that underlie control of feeding behavior. Because AGRP neurons also provide a genetically-accessible entry point into these circuits, we propose that new genetically encoded tools for rapid manipulation of neuronal and synaptic function could be applied to dissect these discrete pathways under normal conditions as well as in pathological states of over- and under-eating.

## Supplementary Material

Refer to Web version on PubMed Central for supplementary material.

## ACKNOWLEDGEMENTS

We thank G. Shtengel for assistance with photostimulation equipment and software, R. Shusterman for assistance with data analysis, H. Peng for image analysis tools, J. Osborne and T. Tabachnik for equipment design and fabrication, A. Arnold for imaging support, B. Shields and A. Hu for histology support, and J. Cox for mouse breeding and genotyping support. K. Svoboda, G. Murphy, J. Dudman, A. Lee, and S.E.R. Egnor commented on the manuscript. This research was funded by the Howard Hughes Medical Institute.

## METHODS

### Animals

All experimental protocols were conducted according to U.S. National Institutes of Health guidelines for animal research and were approved by the Institutional Animal Care and Use Committee at Janelia Farm Research Campus. *Agrp-cre*<sup>18</sup> and *pomc-cre*<sup>19</sup> mice have been described previously. *Agrp-cre;A<sup>y</sup>* and *pomc-cre;A<sup>y</sup>* mice were generated by crossing *agrp-cre* and *pomc-cre* mice, respectively, with heterozygous *A<sup>y</sup>* mice (Jackson Laboratories). Mice were genotyped for *cre* (Transnetyx), and *A<sup>y</sup>* mice were identified by their yellow coat color. Typically, male mice were used. Females were occasionally used for experiments involving *agrp-cre;A<sup>y</sup>* (2/7 mice) and *pomc-cre;A<sup>y</sup>* (3/10 mice); their behavioral responses were not different from results with male mice.

### Stereotaxic viral delivery and fiber guide system implantation

Mice were anaesthetized with isoflurane and were placed into a stereotaxic apparatus (David Kopf Instruments). The skull was exposed via a small incision and a small hole was drilled for injection and fiber guide cannula placement. Mice were injected with virus on only one side of the brain. A pulled glass pipette with 20 – 40 µm tip diameter was inserted into the

brain and two unilateral injections (60 nl) of the rAAV2/rh10-FLEX-*rev*-ChR2-tdTomato virus (titer:  $1.1 \times 10^{13}$  genomic copies/ml, University of Pennsylvania Gene Therapy Program Vector Core; rAAV2-FLEX-*rev*-ChR2-tdTomato plasmid is available from [www.addgene.com](http://www.addgene.com), Plasmid 18917) were made at coordinates around the ARC (bregma: –1.2 mm, midline: +0.2 mm, dorsal surface: –5.85 mm and –5.7 mm). A micromanipulator (Narishige) was used to control the injection speed (30 nl/min), and the pipette was withdrawn 15 min after the final injection. This was followed by insertion of a guide cannula (4.5 mm, 26GA; Plastics One) through the craniotomy. Grip cement (DENTSPLY) was used to anchor the guide cannula to the skull and a dummy cannula (33GA; Plastics One) was inserted to keep the fiber guide from becoming clogged. Mice were returned to their home cage typically for 10 – 14 days to recover and for expression of ChR2:tdtomato.

## Components for food consumption and photostimulation

In the home cage, mice had *ad libitum* access to mouse chow (PicoLab Rodent Diet 20, 5053 tablet, TestDiet). For behavioral testing, mice were transferred into feeding cages (Coulbourn Instruments) and supplied with food pellets (20 mg each) of identical composition to the food in the home cage, delivered by an automatic pellet dispenser. Pellet removal was sensed by the offset of a beam break and an additional pellet was administered after a delay (10 s). Food consumption was monitored continuously by computer using Graphic State (Coulbourn Instruments). Mice also had water available *ad libitum* during behavioral experiments which, in some cases, was monitored by optical detection (Coulbourn Instruments) of licks emitted towards the drinking spout. The mice were allowed to acclimate for 3 days before initiating the photostimulation protocols.

Light was delivered to the brain through an optical fiber. For positioning the fiber, mice were anesthetized with isoflurane the day before photostimulation, and the tip (200  $\mu$ m diameter core; BFH48-200-Multimode, NA 0.48; Thorlabs) was implanted through the fiber guide to a distance of ~0.8 mm from the ARC. The relationship of light scattering and absorption in the brain as a function of distance has been described previously<sup>35</sup>. Using this relationship, the light power exiting the fiber tip (10 mW) was estimated to correspond to 2.0 mW/mm<sup>2</sup> at the ARC, which was sufficient to drive a behavioral response.

For optical delivery of light pulses with millisecond precision to multiple mice, the output from a 200 mW diode laser (Ciel 473 nm, Laser Quantum) was split into four beams using a combination of 50/50 beam splitters and turning mirrors (Thorlabs). Each beam was controlled using an acousto-optic modulator (AOM) (Quanta Tech OPTO-ELECTRONIC) to generate light pulses that were launched into separate fiber ports (PAF-X-7, Thorlabs) and their corresponding optical fibers. Using these components, four mice could be simultaneously and independently photostimulated. Controlling software for the AOMs was written in LabView (National Instruments).

## Behavioral experiments

AGRP-ChR2 and AGRP-ChR2;*A $\gamma$*  mice were tested for evoked feeding behavior during the early light period (lights on at 6:00 a.m.). Food intake was recorded during a pre-stimulus

baseline from 8:00 to 9:00 am followed by a 1 hour photostimulation period from 9:00 to 10:00 am. Afterwards, a post-stimulus period from 10:00 to 11:00 am was also recorded. The primary photostimulation protocol consisted of light pulses (10 ms) for 1 s (20, 10, or 2 Hz) followed by a 3 s break, with the sequence repeating for 1 hour.

We also used a second protocol in which the number of light pulses was kept constant for different stimulation frequencies. Here, 20 light pulses (10 ms each) were delivered for 1 or 8 s (20 or 2.5 Hz), respectively, and the sequence repeated every 10 s for 1 hour. POMC-ChR2 and POMC-ChR2;*A<sup>y</sup>* mice were also tested for evoked feeding behavior. The photostimulation was initiated 1 hour before the onset of the dark period and followed protocol 1 (20 Hz). Stimulation was sustained for 24 hours because an acute reduction of food intake was not typically observed in these mice. Changes in food intake and body weight are reported relative to the mean values over two days prior to photostimulation.

## Histology, imaging and neuron counting

After removing the optical fiber, mice were deeply anaesthetized and then perfused with saline followed by 4% paraformaldehyde (PFA) in phosphate buffered saline and fixed overnight in PFA and transferred to phosphate buffered saline. Brain sections (50  $\mu$ m) were cut by vibratome sectioning, mounted on glass slides using VECTASHIELD mounting medium with DAPI, and coverslipped for imaging. Neuron images were collected by confocal microscopy (Carl Zeiss) using tdTomato fluorescence. Neurons with red fluorescence were counted manually using V3D, an image visualization & analysis software<sup>36</sup>. Ambergrombie's correction<sup>37</sup> was applied to the neuron counts (slice thickness: 50  $\mu$ m, AGRP neuron diameter:  $14 \pm 1$   $\mu$ m, correction factor: 0.78). In the text, neuron counts have been rounded to the nearest hundreds.

## Electrophysiology

Experimental techniques were similar to those reported previously<sup>17</sup>, and only the differences are described here. After viral infection (14 days incubation, viral injection between in P21-25 mice) mice were deeply anaesthetized with isoflurane and decapitated. Coronal brain slices containing the ARC were prepared in chilled cutting solution containing (in mM): 234 sucrose, 28 NaHCO<sub>3</sub>, 7 dextrose, 2.5 KCl, 7 MgCl<sub>2</sub>, 0.5 CaCl<sub>2</sub>, 1 sodium ascorbate, 3 sodium pyruvate and 1.25 mM NaH<sub>2</sub>PO<sub>4</sub>, aerated with 95% O<sub>2</sub>/5% CO<sub>2</sub>. Slices were transferred to artificial cerebrospinal fluid (ACSF) containing (in mM): 119 NaCl, 25 NaHCO<sub>3</sub>, 11 D-glucose, 2.5 KCl, 1.25 MgCl<sub>2</sub>, 2 CaCl<sub>2</sub> and 1.25 NaH<sub>2</sub>PO<sub>4</sub>, aerated with 95% O<sub>2</sub>/5% CO<sub>2</sub>. Slices were incubated at 34 °C for 30 minutes and then maintained and recorded from at room temperature (20–24 °C). Neurons were identified and targeted by tdTomato fluorescence emission (ex: 575 nm, em: 640 nm, dichroic: 610 nm longpass, Chroma, Rockingham, VT). Loose-seal, cell attached recordings (seal resistance: 20 – 70 M $\Omega$ ) in the voltage clamp recording mode with holding current maintained at zero were made using electrodes with tip resistances 4 – 5 M $\Omega$  filled with ACSF. At the end of some recordings tetrodotoxin (1  $\mu$ M, TTX) added to the bath to confirm that the responses were due to voltage gated sodium channels.

## Photostimulation in brain slices

A laser (473 nm, CrystaLaser) was used to deliver light pulses at 0.1 mW. Light pulse duration (10 ms) was controlled by a Pockels cell (ConOptics) and a mechanical shutter (Vincent Associates). A focal spot was targeted onto the specimen with two x-y scanning mirrors (Cambridge Technology) through a 63x microscope objective (Olympus). Laser power was monitored with a photodiode for each light pulse. Neurons were repetitively stimulated for 30 min with bursts of 20 pulses over 1 s followed by either a 2 s (AGRP neurons) or a 3 s (POMC neurons) break. Because 10 ms pulses were used, the possibility existed for two action currents from a single light pulse. This was only observed for  $0.073 \pm 0.005$  % of the total light pulses in AGRP neurons and  $0.66 \pm 0.007$ % of the total light pulses in POMC neurons.

## Electrophysiological analysis

Spikes were detected in a 15 ms window following each photostimulus using the template matching feature in Clampfit (Molecular Devices). The resulting annotations were visually inspected to confirm correct detection.

## Analysis of feeding bouts resulting from photostimulation

We observed that photostimulation-evoked feeding consisted of at least three components occurring at different time scales. The first component was a rapid and regular consumption of pellets. The second component included short interruptions in feeding due to consumption of water or brief investigation of a distractor, after which mice would return to regular food consumption. The third time scale was the intervals during which the animal would rest or groom and pay little attention to food. Here, we calculated feeding bouts to include the first two components. Inter-pellet intervals (IPIs) were log-transformed for all AGRPChR2 mice with greater than 800 ChR2-expressing AGRP neurons. The frequency distribution of log(IPIs) was fit to a double log-normal model<sup>22</sup> (Supplementary Fig. 4):

$$y = A_1 * \exp\left(-\frac{(t - \mu_1)^2}{2\sigma_1^2}\right) + A_2 * \exp\left(-\frac{(t - \mu_2)^2}{2\sigma_2^2}\right) \quad \text{Eq(1)}$$

Where  $y$  is the frequency distribution of log-transformed intervals with length  $t$ ,  $\mu_1$  and  $\mu_2$  are the mean log(IPIs) of the two IPI groups,  $\sigma_1$  and  $\sigma_2$  are the standard deviation of the two IPI groups,  $A_1$  and  $A_2$  reflect the modeled peak frequencies of the two IPI components.

A threshold value for a feeding bout was calculated:

$$\text{threshold} = \text{antilog}(\mu_2 + 3 * \sigma_2) \quad \text{Eq(2)}$$

Bout duration and consumption was determined by applying this threshold (2.4 min) to the photostimulation-evoked food consumption curves for individual AGRP-ChR2 mice. Inspection of the bouts with respect to IPIs showed that the thresholding approach produced meaningful bouts for 1 hour continuous stimulation (Supplementary Fig. 5) as well as for stimulation that was ceased only 5 minutes after the first pellet was taken (Supplementary Fig. 6). Bout duration was the time from the consumption of the first pellet to the last pellet

with IPI < threshold and bout consumption was the number of pellets consumed for each animal over this time.

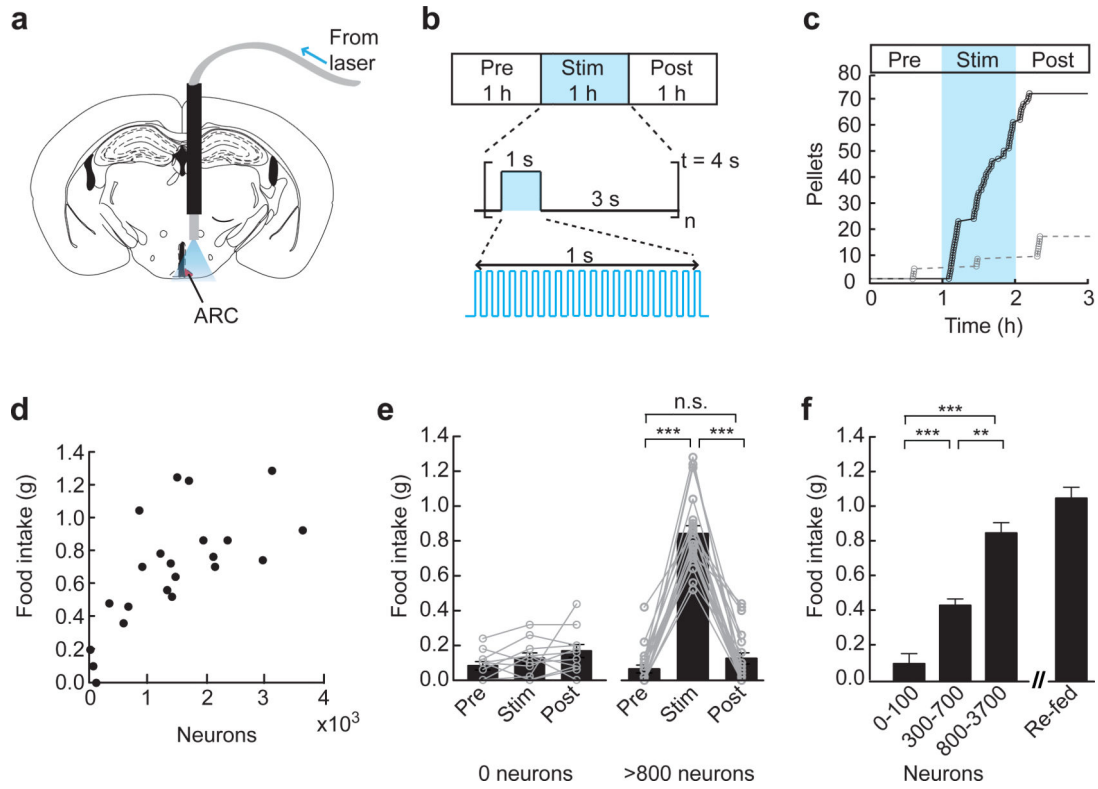
## Statistical analysis

Values are reported as mean  $\pm$  s.e.m., and error bars are s.e.m. Linear and nonlinear curve fitting was performed using the Curve Fitting Toolbox in Matlab (Mathworks). Statistical tests were paired or unpaired *t*-tests and multiple comparisons were corrected by Holm's method<sup>38</sup>.

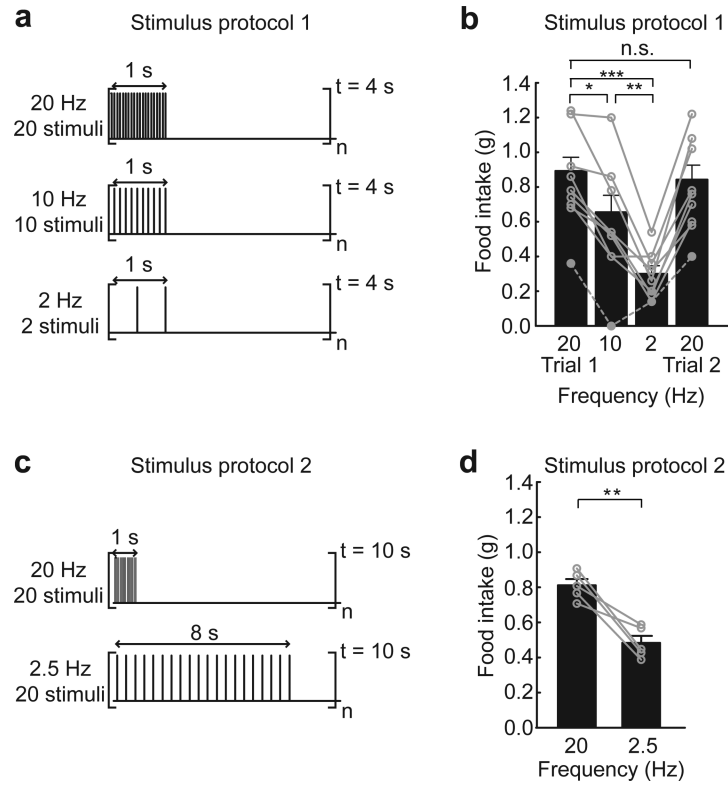
## References

1. Morton GJ, Cummings DE, Baskin DG, Barsh GS, Schwartz MW. Central nervous system control of food intake and body weight. *Nature*. 2006; 443:289–295. [PubMed: 16988703]
2. Ollmann MM, et al. Antagonism of central melanocortin receptors in vitro and in vivo by agouti-related protein. *Science*. 1997; 278:135–138. [PubMed: 9311920]
3. Clark JT, Kalra PS, Crowley WR, Kalra SP. Neuropeptide Y and human pancreatic polypeptide stimulate feeding behavior in rats. *Endocrinology*. 1984; 115:427–429. [PubMed: 6547387]
4. Levine AS, Morley JE. Neuropeptide Y: a potent inducer of consummatory behavior in rats. *Peptides*. 1984; 5:1025–1029. [PubMed: 6549409]
5. Stanley BG, Leibowitz SF. Neuropeptide Y: stimulation of feeding and drinking by injection into the paraventricular nucleus. *Life Sci*. 1984; 35:2635–2642. [PubMed: 6549039]
6. Takahashi KA, Cone RD. Fasting induces a large, leptin-dependent increase in the intrinsic action potential frequency of orexigenic arcuate nucleus neuropeptide Y/Agouti-related protein neurons. *Endocrinology*. 2005; 146:1043–1047. [PubMed: 15591135]
7. Tsujii S, Bray GA. Acetylation alters the feeding response to MSH and beta-endorphin. *Brain Res Bull*. 1989; 23:165–169. [PubMed: 2555029]
8. Yaswen L, Diehl N, Brennan MB, Hochgeschwender U. Obesity in the mouse model of pro-opiomelanocortin deficiency responds to peripheral melanocortin. *Nat Med*. 1999; 5:1066–1070. [PubMed: 10470087]
9. Cowley MA, et al. Leptin activates anorexigenic POMC neurons through a neural network in the arcuate nucleus. *Nature*. 2001; 411:480–484. [PubMed: 11373681]
10. Roseberry AG, Liu H, Jackson AC, Cai X, Friedman JM. Neuropeptide Y-mediated inhibition of proopiomelanocortin neurons in the arcuate nucleus shows enhanced desensitization in ob/ob mice. *Neuron*. 2004; 41:711–722. [PubMed: 15003171]
11. Cowley MA, et al. Electrophysiological actions of peripheral hormones on melanocortin neurons. *Ann N Y Acad Sci*. 2003; 994:175–186. [PubMed: 12851314]
12. Luquet S, Perez FA, Hnasko TS, Palmiter RD. NPY/AgRP neurons are essential for feeding in adult mice but can be ablated in neonates. *Science*. 2005; 310:683–685. [PubMed: 16254186]
13. Wu Q, Howell MP, Cowley MA, Palmiter RD. Starvation after AgRP neuron ablation is independent of melanocortin signaling. *Proc Natl Acad Sci U S A*. 2008
14. Wu Q, Boyle MP, Palmiter RD. Loss of GABAergic signaling by AgRP neurons to the parabrachial nucleus leads to starvation. *Cell*. 2009; 137:1225–1234. [PubMed: 19563755]
15. Boyden ES, Zhang F, Bamberg E, Nagel G, Deisseroth K. Millisecond-timescale, genetically targeted optical control of neural activity. *Nat Neurosci*. 2005; 8:1263–1268. [PubMed: 16116447]
16. Li X, et al. Fast noninvasive activation and inhibition of neural and network activity by vertebrate rhodopsin and green algae channelrhodopsin. *Proc Natl Acad Sci U S A*. 2005; 102:17816–17821. [PubMed: 16306259]
17. Atasoy D, Aponte Y, Su HH, Sternson SM. A FLEX switch targets Channelrhodopsin-2 to multiple cell types for imaging and long-range circuit mapping. *J Neurosci*. 2008; 28:7025–7030. [PubMed: 18614669]

18. Kaelin CB, Xu AW, Lu XY, Barsh GS. Transcriptional regulation of agouti-related protein (Agrp) in transgenic mice. *Endocrinology*. 2004; 145:5798–5806. [PubMed: 15345681]
19. Balthasar N, et al. Leptin receptor signaling in POMC neurons is required for normal body weight homeostasis. *Neuron*. 2004; 42:983–991. [PubMed: 15207242]
20. van den Top M, Lee K, Whyment AD, Blanks AM, Spanswick D. Orexigen-sensitive NPY/AgRP pacemaker neurons in the hypothalamic arcuate nucleus. *Nat Neurosci*. 2004; 7:493–494. [PubMed: 15097991]
21. Tolkamp BJ, Allcroft DJ, Austin EJ, Nielsen BL, Kyriazakis II. Satiety splits feeding behaviour into bouts. *J Theor Biol*. 1998; 194:235–250. [PubMed: 9778436]
22. Tolkamp BJ, Kyriazakis II. To split behaviour into bouts, log-transform the intervals. *Anim Behav*. 1999; 57:807–817. [PubMed: 10202089]
23. Miller MW, et al. Cloning of the mouse agouti gene predicts a secreted protein ubiquitously expressed in mice carrying the lethal yellow mutation. *Genes Dev*. 1993; 7:454–467. [PubMed: 8449404]
24. Kristensen P, et al. Hypothalamic CART is a new anorectic peptide regulated by leptin. *Nature*. 1998; 393:72–76. [PubMed: 9590691]
25. Elias CF, et al. Leptin activates hypothalamic CART neurons projecting to the spinal cord. *Neuron*. 1998; 21:1375–1385. [PubMed: 9883730]
26. Rossi M, et al. A C-terminal fragment of Agouti-related protein increases feeding and antagonizes the effect of alpha-melanocyte stimulating hormone in vivo. *Endocrinology*. 1998; 139:4428–4431. [PubMed: 9751529]
27. Fan W, Boston BA, Kesterson RA, Hruby VJ, Cone RD. Role of melanocortinergic neurons in feeding and the agouti obesity syndrome. *Nature*. 1997; 385:165–168. [PubMed: 8990120]
28. Huber D, et al. Sparse optical microstimulation in barrel cortex drives learned behaviour in freely moving mice. *Nature*. 2008; 451:61–64. [PubMed: 18094685]
29. Houweling AR, Brecht M. Behavioural report of single neuron stimulation in somatosensory cortex. *Nature*. 2008; 451:65–68. [PubMed: 18094684]
30. Tsai HC, et al. Phasic firing in dopaminergic neurons is sufficient for behavioral conditioning. *Science*. 2009; 324:1080–1084. [PubMed: 19389999]
31. Adamantidis AR, Zhang F, Aravanis AM, Deisseroth K, de Lecea L. Neural substrates of awakening probed with optogenetic control of hypocretin neurons. *Nature*. 2007; 450:420–424. [PubMed: 17943086]
32. Abbott SB, et al. Photostimulation of retrotrapezoid nucleus phox2b-expressing neurons in vivo produces long-lasting activation of breathing in rats. *J Neurosci*. 2009; 29:5806–5819. [PubMed: 19420248]
33. Belgardt BF, Okamura T, Bruning JC. Hormone and glucose signalling in POMC and AgRP neurons. *J Physiol*. 2009; 587:5305–5314. [PubMed: 19770186]
34. Broberger C, Johansen J, Johansson C, Schalling M, Hokfelt T. The neuropeptide Y/agouti gene-related protein (AGRP) brain circuitry in normal, anorectic, and monosodium glutamate-treated mice. *Proc Natl Acad Sci U S A*. 1998; 95:15043–15048. [PubMed: 9844012]
35. Aravanis AM, et al. An optical neural interface: in vivo control of rodent motor cortex with integrated fiberoptic and optogenetic technology. *J Neural Eng*. 2007; 4:S143–156. [PubMed: 17873414]
36. Peng H, Ruan Z, Long F, Simpson JH, Myers EW. V3D enables real-time 3D visualization and quantitative analysis of large-scale biological image data sets. *Nat Biotechnol*. 28:348–353. [PubMed: 20231818]
37. Abercrombie M. Estimation of nuclear population from microtome sections. *Anat. Rec*. 1946; 94:239–247. [PubMed: 21015608]
38. Holm SA. A simple sequentially rejective multiple test procedure. *Scand. J. Statist*. 1979; 6:65–70.



**Figure 1.** AGRP neurons are sufficient to evoke voracious food consumption in well-fed mice. **(a)** For light delivery, an optical fiber was implanted ~0.8 mm above the arcuate nucleus (ARC, red). **(b)** Experimental design. Food intake was recorded before, during and after photostimulation. The stimulus was applied repeatedly over 1 second followed by a 3 second break. Photostimulation frequency was 20 Hz with 10 ms light pulses. **(c)** Photostimulation in an AGRP-ChR2 mouse evoked voracious food consumption during the stimulation period (black trace) but not in a mouse without ChR2 expression (grey trace). **(d)** Food intake was dependent on the number of ChR2-expressing AGRP neurons. Circles represent 1 hour food intake for individual mice ( $n = 22$ ). **(e)** Mice without ChR2 expression in AGRP neurons ( $n = 11$ ) did not show a significant difference in food intake during photostimulation, whereas in mice with greater than 800 ChR2-expressing neurons ( $n = 16$ ) the increase in food intake during photostimulation was significant. Circles connected by lines represent food intake for individual mice. **(f)** Food intake during photostimulation was significantly increased in mice with intermediate (300–700 neurons;  $n = 3$ ) or high levels of ChR2 expression (>800 neurons;  $n = 16$ ) relative to mice with low or no ChR2 (0–100 neurons;  $n = 14$ ). Photostimulation-induced food consumption was nearly as great as the magnitude of re-feeding ( $n = 9$ ) for 1 hour after 24 hours of food deprivation. n.s., not significant; \*\*  $P < 0.01$ ; \*\*\*  $P < 0.001$ . Error bars represent s.e.m.

**Figure 2.**

AGRP neuron-evoked feeding is dependent on the stimulation frequency. **(a)** Stimulus protocol 1. Bursts of light pulses were applied for 1 s followed by a 3 s break which repeated continuously for 1 hour. Within the burst, frequency (Hz) and number (pulses) was varied between 20, 10, 2, and 20 on successive days for AGRP-ChR2 mice. **(b)** Dependence of food intake on stimulation frequency (stimulus protocol 1) for mice with greater than 800 ChR2-expressing neurons ( $n = 8$ ). As the stimulus frequency was reduced, feeding decreased. Grey dashed trace shows example of a mouse with intermediate ChR2 expression (600 neurons, not included in sample mean) which had a similar relationship. On the final day, food intake was measured again in response to a second 20 Hz stimulation trial and was found to be similar to the consumption from the first day. Circles represent food intake for individual mice. **(c)** Stimulus protocol 2. Bursts of 20 light pulses were delivered every 10 s such that 20 Hz and 2.5 Hz stimulation frequencies could be applied while maintaining the same number of stimuli over the 1 hour stimulation epoch. **(d)** Mice that received different stimulus frequencies (20 and 2.5 Hz) but the same total number of stimuli over 1 hour (stimulus protocol 2) also showed a reduction in food intake with decreasing stimulus frequency ( $n = 5$ ). n.s., not significant; \*  $P < 0.05$ ; \*\*  $P < 0.01$ ; \*\*\*  $P < 0.001$ . Error bars represent s.e.m.

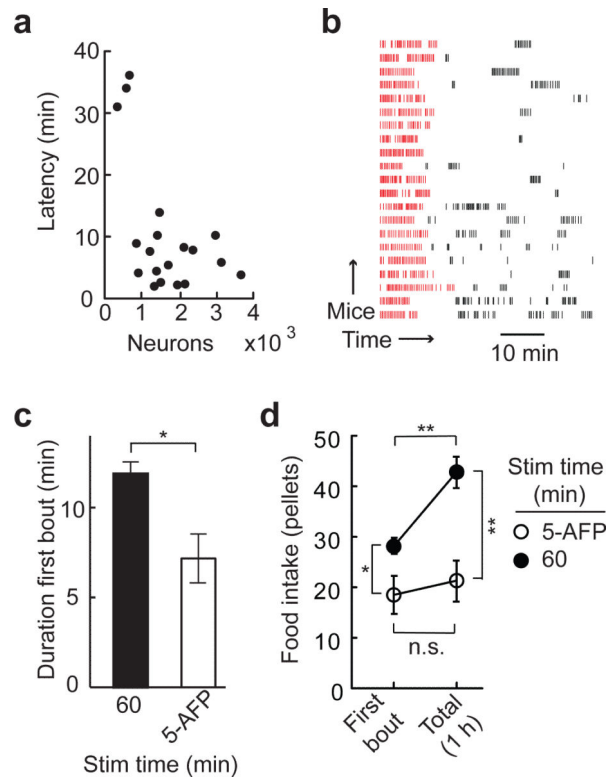


**Figure 3.**

AGRP neuron-evoked feeding is rapidly initiated by stimulus onset and terminated after its offset. **(a)** Latency to food intake after photostimulation onset for each mouse (circles,  $n = 19$ ). **(b)** For AGRP-ChR2 mice with greater than 800 ChR2-expressing neurons, raster plot of food intake aligned to the first pellet shows an initial feeding bout (red ticks) and more variable subsequent bouts (black ticks). Each row is from an individual mouse. **(c)** The duration of the first bout during continuous photostimulation (filled bar,  $n = 16$ ) is reduced when stimulation is terminated 5 min after the first pellet (AFP) is taken (empty bar,  $n = 5$ ). **(d)** Food intake for the first bout and over a 60 min period for mice continuously stimulated for 1 hour (filled circles) and mice in which stimulation is terminated 5 min AFP (empty circles). n.s., not significant; \*  $P < 0.05$ ; \*\*  $P < 0.01$ . Error bars represent s.e.m.

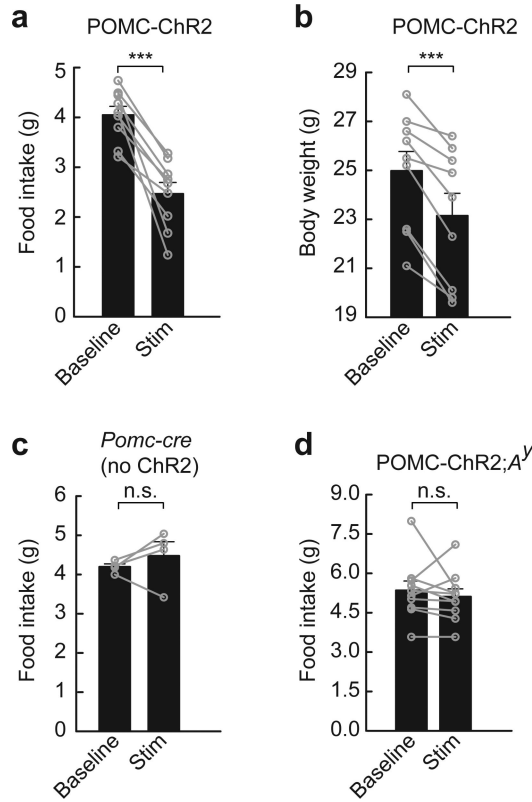


**Figure 4.** POMC neurons inhibit food intake and body weight through melanocortin receptors. **(a,b)** Photostimulation of POMC neurons (20 Hz, protocol 1 extended for 24 hours) leads to reduction of **(a)** food intake and **(b)** body weight ( $n = 9$ ). **(c)** *Pomc-cre* mice without ChR2 expression in POMC neurons ( $n = 4$ ) did not show a significant change in food intake over 24 hours of photostimulation. **(d)** In POMC-ChR2;*A<sup>y</sup>* mice, hypophagia from POMC neuron activation was blocked by *agouti* antagonism of melanocortin signaling ( $n = 10$ ). Baseline refers to average food intake or body weight for the two days prior to photostimulation. n.s., not significant; \*\*\*  $P < 0.001$ . Error bars represent s.e.m.

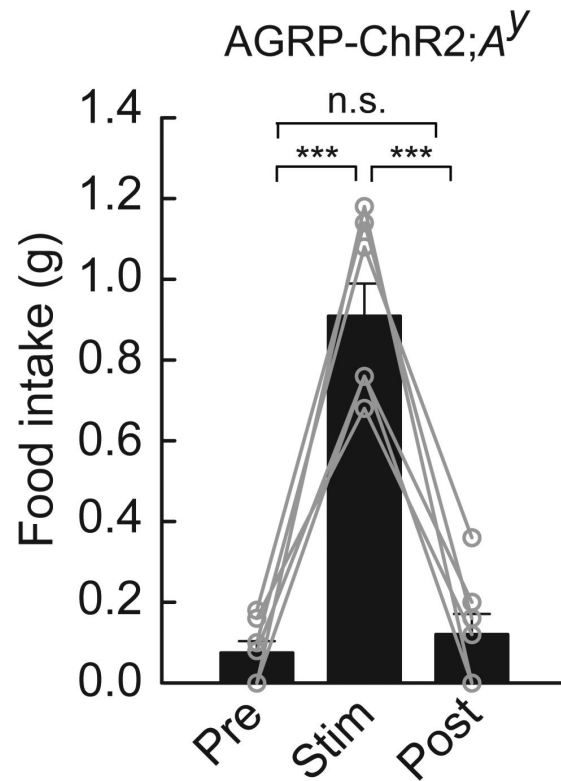


**Figure 5.** Evoked feeding does not require melanocortin suppression. Photostimulation of AGRP-ChR2;A<sup>y</sup> mice evoked avid food intake, indicating that AGRP neurons can promote feeding independently of melanocortin receptor suppression ( $n = 7$ ). n.s., not significant; \*\*\*  $P < 0.001$ . Error bars represent s.e.m.